Signal Processing in Insect Hearing Organs

A. Kern * R. Stoop * M. Göpfert † D.A. Smirnov ‡ B.B. Bezrucko ‡

Abstract — **Many insects are endowed with small, yet very powerful hearing organs whose signal processing characteristics are very similar to those of the mammalian cochlea. We investigate self-sustained oscillation (SO) data of the *Drosophila* hearing organ and demonstrate that they are faithfully described by a generalized van-der-Pol system. Technical applications may benefit from a profound understanding of this compact and sensitive sound detector.**

1 INTRODUCTION

The proportion of people suffering from cochlear hearing loss is ever increasing in industrialized countries, and its treatment by hearing aids is often not satisfactory. This situation can be improved if the principles of auditory processing are understood. This knowledge may then be used for hearing-aid design. Other electronic sound processing systems, such as speech recognition devices, also benefit from this biomorphic approach [1].

Up to now, research was mostly focused on the mammalian cochlea. In addition to physiological investigations, models of the cochlea have been devised in order to gain insight into the fundamental principles of hearing [2, 3]. Cochlear signal processing has also been implemented as electronic circuits (*silicon cochlea*) [4, 5]. The hearing organs of many insects, however, exhibit the same signal processing characteristics as the mammalian cochlea [6]: They are able to actively amplify an incoming stimulus, display a pronounced compressive nonlinearity, and are able to generate self-sustained oscillations (SO) in the absence of any sound. SO are the counterpart to spontaneous otoacoustic emissions (SOAE) of the mammalian cochlea. Prestin, which is the fifth member of the anion transporter family SLC26, has been identified as the molecular motor for amplification in the mammalian cochlea. In the hearing organs of *Drosophila*, a prestin-related protein of the SLC26 family is expressed [7]. From these findings it is concluded in [7] that the outer hair cells in mammals and the insect auditory sensors may have their common evolutionary origin in ancient mechanosensory cells. The fundamental mechanisms of active amplification are thus most likely similar in both mammals and insects.

Since insect hearing organs are located on the body surface, they are, in contrast to the mammalian cochlea, accessible to non-invasive measurement; furthermore, simultaneous recordings of the neural activity are possible. Therefore, research on the insect auditory system will provide profound insights into the principles of auditory information processing. Since insect hearing organs are – despite their smallness – very powerful and often very specialized, their understanding may pave the way towards miniaturized artificial acoustic sensors.

In this contribution, we will investigate SO in the hearing organ of *Drosophila melanogaster*. By using time-series analysis methods, we will reconstruct the generating differential equation. We will show that the SO, and thus the amplification process, are governed by a generalized van-der-Pol equation. The *Drosophila* hearing system is thus driven by a superregenerative amplifier, in agreement with a hypothesis originally brought forward by Gold in 1948 [8] for the mammalian cochlea.

2 LIMIT-CYCLE OSCILLATIONS IN THE DROSOPHILA HEARING ORGAN

2.1 The *Drosophila* Hearing Organ

Insect hearing organs, which occur in a large variety and at different places on the insect body (head, thorax, legs etc.), are divided into two classes [9]: (1) tympanal hearing organs, which detect the sound pressure variations of the acoustic far-field, and (2) detectors for the acoustic near field, which are responsive to air particle velocity, and whose frequency range is restricted to below $\sim$ 1000 Hz. The *Drosophila* antenna, which operate as a sound receiver, belong to the latter class.

An incoming sound stimulus induces vibrations in the most distal part of the fly's antenna, the feathery *arista*. These vibrations are transmitted to *Johnston's organ* in the antenna's basal part, the hearing organ proper, where the mechanical vibrations are transduced into neural excitations. Johnston's organ consists of hundreds of mechanoreceptor units, and it is the origin of the active amplification process.

*Institute of Neuroinformatics, University / ETH Zürich, Winterthurerstr. 190, 8057 Zürich, Switzerland, e-mail: [albert,ruedi]@ini.phys.ethz.ch, tel.: +41 1 635 30 66

†Zoologisches Institut, Universität zu Köln, Weyertal 119, 50923 Köln, Germany

‡Laboratory of Dynamical Modeling and Diagnostics, Saratov State University, 155 Moskovskaya Street, Saratov 410026, Russia, e-mail: bbp@sgu.ru

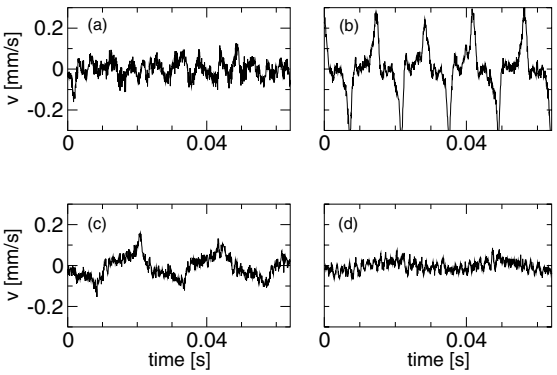

Figure 1: SO of *Drosophila* (antenna velocity). (a) 10 min, (b) 20 min, (c) 30 min, (d) 34 min after DMSO injection.

2.2 Autonomous Vibrations

In the absence of any sound, SO can be induced by injection of dimethylsulphoxide (DMSO), and may last for up to $1-1.5$ hours. DMSO is a local analgesic which is known to affect insect mechanosensory receptors. The precise mechanism by which DMSO induces SO is still unclear. However, as DMSO-induced SO are metabolically vulnerable (the are reversibly suppressed by CO_2 exposure), they must be related to the active amplification mechanism [6]. From SO measurements, insights into the amplification process may thus be gained.

The fully developped SO appear about 20 min after injection (Fig. 1 (b)) and have the shape of relaxation oscillations, with a characteristic frequency of about 100 Hz. After another 10 min (Fig. 1 (c)), the SO amplitudes decrease, and in the further course of time, when the DMSO concentration has significantly decreased, the SO approach a sinusoidal form Fig. 1 (d).

These observations are reminiscent of limit-cycle oscillations of the van-der-Pol type,

$$\ddot{x} - \mu(1 - x^2)\dot{x} + x = 0, \qquad (1)$$

which appear if the control parameter $\mu > 0$ is decreased, starting from a high value (x denotes the antenna location). Note that for $\mu > 0$, undamping (i.e. amplification) occurs for small x, and stable limit cycles emerge. However, the pronounced asymmetry visible in Fig. 1 (b) (compare onset and extent of upward and downward excursions within one period), which is gradually reduced at later times (Figs. 1 (c) and (d)), necessitates a more general model for SO generation. Instead of (1), we therefore hypothesize the more general system

$$\ddot{x} - P_n(x)\dot{x} + P_m(x) = 0, \qquad (2)$$

where, since antenna vibrations are continuous, we choose a polynomial ansatz (of order n and m, respectively) for the functions $P_n(x)$ and $P_m(x)$. $P_n(x)$ thus describes the nonlinear, and possibly negative, friction, and $P_m(x)$ denotes the nonlinear restoring force.

In the following section n, m and the polynomial coefficients are determined. If the model (2) is realistic, the polynomial orders n and m can unambiguously be determined. Moreover, variation of the coefficients with time (i.e. with decreasing DMSO concentration) will then account for the observed variation of SO shapes.

3 MODEL CONSTRUCTION

3.1 Numerical Differentiation and Integration

From the measurements, we are given a time series of antenna velocities. For the model reconstruction (see Sec. 3.2), we also need the antenna locations and accelerations. These are determined by numerical differentiation and integration, respectively.

For both methods some difficulties must be overcome. Slow changes in the mean antenna velocity induce a significant drift in the computed (by numerical integration) antenna locations. This drift can be excluded by approximating the computed locations by a polynomial in the least-squares sense. If a polynomial of 20th order is used, it is sufficient to drop the linear and quadratic trend. However, such high-order polynomials induce oscillations near the beginning and end of the time series. These characteristic periods at the edges of the time series must be neglected in the further analysis.

For applying numerical differentiation, the measured noisy time series must be smoothed in order to reduce the effects of the noise. This was achieved by applying a first order Savitsky-Golay filter [10].

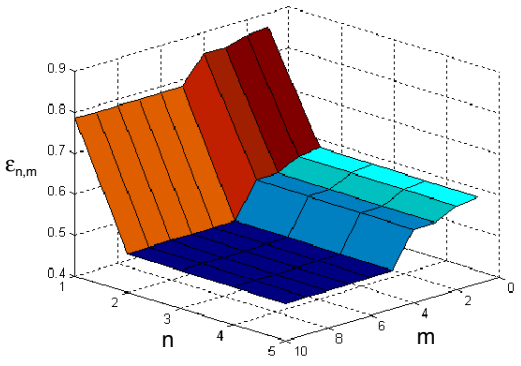

Figure 2: Mean-squared error $\epsilon^2_{n,m}$ of model fitting (see (5)).

3.2 Van-der-Pol Model

Let us assume that the model that generates the measured time series is given by the differential equation

$$\ddot{x} = f(x, \dot{x}). \tag{3}$$

Under the hypothesis that the SO constitute van-der-Pol oscillations of the form (2), we set

$$f(x, \dot{x}) = P_n(x)\dot{x} - P_m(x). \tag{4}$$

In order to determine the polynomial orders n and m, the polynomial coefficients are fitted such that the squared error

$$\epsilon^2_{n,m} = \sum_{i=1}^{N} \left(\ddot{x}(t_i) - f(x(t_i), \dot{x}(t_i))\right)^2, \tag{5}$$

is minimized. Since the time series is non-stationary, the time steps t_i, at which $\dot{x}(t_i)$ is measured, should encompass only a quasistationary subset of the entire time series. The length N of these subsets ($\sim$ 4000 data points) is large enough so that polynomial fitting can be reliably performed.

It is observed that the error $\epsilon^2_{n,m}$ saturates for $n = 2$ and $m = 5$ (Fig. 2). A further increase of $\{n, m\}$ does not reduce $\epsilon^2_{n,m}$. The emergence of such a conspicuous saturation point is remarkable. It is a very rare case and may indicate that the model structure (2) is adequate to the *Drosophila* auditory system. On the other hand, the relatively high noise level may possibly prevent the error $\epsilon^2_{n,m}$ from decreasing any further. In the absence of noise, the errors may thus gradually decrease with increasing $\{n, m\}$. A careful application of noise-cleaning methods [11] to the time series, before the model (2) is fitted, will provide evidence whether this will be the case.

However, the rapid decay of $\epsilon_{n,m}$ before saturation indicates that the chosen model structure (2) is realistic. A comparison between realizations of time series by the model and the measurements for

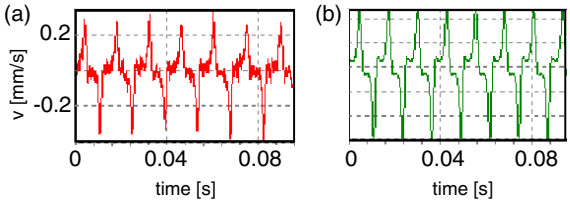

Figure 3: (a) Flagellum velocity observed 20 min after DMSO injection (fully developped SO). (b) Realization of a time series by the model (2), using $n = 2$ and $m = 5$.

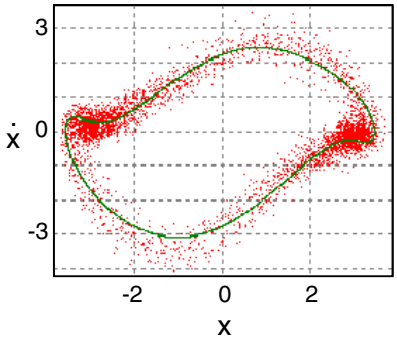

Figure 4: Phase-space representation of measured (dots) and modelled (solid line) antennal vibrations (at fully developped SO).

fully developped SO (20 min after DMSO injection; see Fig. 3) reveals that the measured antenna velocities are indeed faithfully reproduced. This is even better visible in Fig. 4, where modelled and measured data are compared in the phase plane $(x, \dot{x})$ (note that the antenna positions x are obtained by numerical integration from measured velocities; see Sec. 3.1).

4 AMPLIFICATION DYNAMICS

The asymmetry of the observed antenna oscillations when SO are fully developped (cf. Fig. 1 (a)) is reflected in the shape of $P_n(x)$ and $P_m(x)$. It is seen that $P_n(x)$ becomes negative for small excursions x (Fig. 5 (a)). Since $P_n(x)$ represents nonlinear friction, $P_n(x) < 0$ signifies that energy is injected into the system. This is characteristic for the operation of an active amplification process.

The nonlinear restoring force $P_m(x)$ displays a more pronounced asymmetry than $P_n(x)$ (Fig. 5 (b)). $P_m(x)$ and its first derivatives are small around $x = 0$. This means that for small antenna displacements, only a small restoring force is present. The system is thus easily driven to relatively large amplitudes by the negative friction term. The asymmetry of both $P_n(x)$ and $P_m(x)$ becomes effective at large displacements and may have its origin in geometrical properties of the fly's antenna.

In the course of time, i.e. with decreasing DMSO concentration, the nonlinear contributions to friction and restoring force decay. In particular, the range where friction becomes negative gradually decreases and finally vanishes, in agreement with the observed reduction in SO amplitude (see Fig. 1). Interestingly, in addition to becoming approximately linear in the absence of SO, the restoring force function $P_m(x)$ also becomes very flat. Sim-

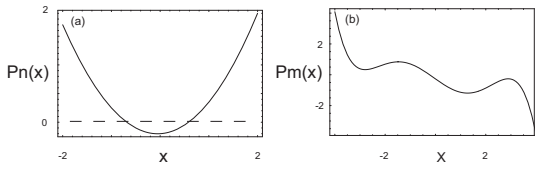

Figure 5: (a) Nonlinear friction $P_n(x)$, (b) nonlinear restoring force $P_m(x)$ ($n = 2$, $m = 5$; 20 min after DMSO injection, fully developped SO).

ilarly, the friction term remains very small. This indicates that the system is very responsive. Even a very faint incoming stimulus thus would rapidly elicit antenna vibrations. Although the amplifier has now returned to a stable state, where limit-cycles do not occur, it remains very sensitive. Only small parameter variations are necessary to render the friction term negative and thereby amplify incoming vibrations.

Our results may be compared to measurements of hair-bundle stiffness in lower vertebrates [12]. In the hearing organs of amphibia and reptiles, amplification is achieved by active hair-bundle movements. Mechanical stimulation of hair bundles revealed that the bundle stiffness may become *negative* for small bundle displacements [12]. Bundle stiffness has its origin in ion-channel dynamics, which is considered the source of active amplification. In our analysis amplification is generated by negative friction, in contrast to negative stiffness.

Recently, it was proposed that active amplification in the mammalian hearing system is governed by the generic Hopf-type differential equation [13]. It was later demonstrated that a Hopf-type cochlea model [3] is able to faithfully reproduce measured cochlea responses. Furthermore, the cochlear processing of multi-frequency tones is easily explained in this way [14]. Note that also the van-der-Pol system exhibits a Hopf bifurcation at $\mu = 0$. Active amplification by using the characteristics of a Hopf bifurcation may thus constitute a general, and early developed, mechanism.

5 CONCLUSIONS

DMSO-induced SO reflect fundamental characteristics of active amplification in the *Drosophila* hearing organ. Their shape and variation in time are faithfully modelled by a generalized van-der-Pol equation, and the saturation properties in model-fitting are a hint that this model is accurate. In its normal state, the *Drosophila* hearing system is able to deal with the problem of internal noise (in contrast to van-der-Pol based radio amplifiers). In order to find out more about the active amplification properties under normal conditions (i.e. in the absence of SO), further measurements must be performed. In particular, simultaneous neuronal recordings would be of great value.

References

[1] J. Tchorz, B. Kollmeier, "A model of auditory perception as front end for automatic speech recognition", J. Acoust. Soc. Am., vol. 106, pp. 2040–2050, 1999.

[2] P. Dallos, A.N. Popper, R.R. Fay (eds.), "The Cochlea. Springer Handbook of Auditory Research", Springer, 1996.

[3] A. Kern, R. Stoop, "Essential role of couplings between hearing nonlinearities", Phys. Rev. Lett., vol. 91, pp. 128101 1–4, 2003.

[4] J.-J. van der Vyver, A. Kern, R. Stoop, "Active component implementation of a biomorphic Hopf cochlea", Proc. of the European Conference on Circuit Theory and Design ECCTD, pp. 285–288, 2003.

[5] R. Sarpeshkar, R.F. Lyon, C.A. Mead, "A Low-Power Wide-Dynamic-Range Analog VLSI Cochlea", Analog Integrated Circuits and Signal Processing, vol. 16, pp. 245–274, 1998.

[6] M. Göpfert, D. Robert, "Motion generation by *Drosophila* mechanosensory neurons", Proc. Natl. Acad. Sci. U.S.A., vol. 100, pp. 5514–5519 (2003).

[7] T. Weber et al., "Expression of prestin-homologous solute carrier (SLC26) in auditory organs of non-mammalian vertebrates and insects", Proc. Natl. Acad. Sci. U.S.A., vol. 100, pp. 7690–7695, 2003.

[8] T. Gold, "Hearing. II. The physical basis of the action of the cochlea", Proc. R. Soc. Lond. B, vol. 135, pp. 492–498, 1948.

[9] R.R. Hoy, A.N. Popper, R.R. Fay (eds.), "Comparative Hearing: Insects. Springer Handbook of Auditory Research", Springer, 1998.

[10] A. Savitsky, M.J.E. Golay, "Smoothing and differentiation of data by simplified least square procedures", Anal. Chem., vol. 36, pp. 1627–1639, 1964.

[11] A. Kern, W.-H. Steeb, R. Stoop, "Projective noise cleaning with dynamic neighborhood selection", Int. J. Mod. Phys. C, vol. 11, pp. 125–146, 2000.

[12] P. Martin, A.D. Mehta, A.J. Hudspeth, "Negative hair-bundle stiffness betrays a mechanism for mechanical amplification by the hair cell", Proc. Natl. Acad. Sci. U.S.A., vol. 97, pp. 12026–12031, 2000.

[13] V.M. Eguíluz et al., "Essential nonlinearities in hearing", Phys. Rev. Lett., vol. 84, pp. 5232–5235, 2000.

[14] R. Stoop, A. Kern, "Two-tone suppression and combination tone generation as computations performed by the Hopf cochlea", Phys. Rev. Lett., vol. 93, pp. 268103 1–4, 2004.